MODE I FRACTURE TOUGHNESS BEHAVIOUR OF EPOXY RESIN-CARBON FIBER COMPOSITES CURED BY IONISING RADIATION

G. Pitarresi[1*], D. Tumino[2], S. Alessi[1], A. Nowicki[3], G. Spadaro[1]

[1] *Dipartimento di Ingegneria Chimica, Gestionale, Informatica, Meccanica - Università degli Studi di Palermo, Viale delle Scienze, 90128 Palermo, Italy*
[2] *Facoltà di Ingegneria, Architettura e delle Scienze motorie, Università degli Studi di Enna "Kore", Cittadella Universitaria, 94100 Enna, Italy*
[3] *Inst. of Nuclear Chemistry and Technology (ICHTJ), Dorodna 16, 03-195 Warsaw, Poland*
** giuseppe.pitarresi@unipa.it*

Keywords: Radiation Curing, CFRP, Delamination Fracture Toughness, Dynamic Mechanical Thermal Analysis.

Abstract

In this work Mode I fracture toughness behavior of Electron Beam cured unidirectional CFRP laminates is investigated by means of standardized Double Cantilever Beam (DCB) tests. A matrix system, comprising a DGEBA epoxy monomer and a typical initiator of cationic polymerization, was used and panel samples assembled by hand lay-up. Curing was achieved by 20 to 40 minutes irradiation on a pulsed 10 MeV Electron Beam accelerator. One batch of resin was also mixed with 10 phr of a PES thermoplastic monomer in order to enhance the matrix toughness. The influence of fibre-matrix adhesion, matrix toughening and matrix crosslinking density on the mode I delamination behavior have been investigated by correlating the results of DCB and Dynamic Mechanical Thermal Analysis (DMTA) tests.

1 Introduction

Exposure to ionizing radiation represents an alternative way to the conventional thermal curing processes to produce advanced fibre-reinforced polymer (FRP) composites [1]. Some attractive advantages of this out-of-autoclave process comprise the possibility to manufacture complex parts at relatively low temperatures and short times, save in equipment maintenance costs and enhance environmental sustainability (e.g. by a reduced use and exposure to hazardous additives and volatiles, and lower processing energy consumption).

In the last two decades several studies have focused on the adaptation of suitable polymer chemistry to enable radiation induced cross-linking polymerisation [1-3]. Joined network research programmes have also demonstrated the possibility to adapt radiation facilities to manufacture industrial grade large and complex FRP composite parts [2-4], and r&d projects are in course within the aerospace sector trying to exploit all the know-how acquired so far [5,6]. A common aim and key aspect of most studies on radiation curing of bulk resin systems has been the optimisation of materials and process parameters in order to achieve adequate, controlled and reproducible all-round physical and mechanical performances. In this perspective several studies have been focused on the development of multifunctional nano and micro structured resin systems [7,8]. Two topics in particular have received attention: the achievement of high cross-linking density, and the enhancement of matrix fracture toughness, e.g. by opportune tuning of structural morphology through the addiction of nano and micro-

phases [8]. While considering bulk matrices these studies have demonstrated the possibility to match or even improve performances of equivalent thermally cured systems, when it comes to consider fibre reinforced matrix systems a major weakness has been identified in the quality of fibre-matrix adhesion [9-11]. Indeed the low fibre-matrix adhesion strength is perceived by many researchers as a major key barrier limiting the more widespread adoption of radiation curing by the aerospace industry [11]. In fact some most important damage mechanisms leading to failure in FRP composites usually arise when off-axis structural response is solicited. In this situation the overall behaviour is dominated by both the matrix and the fibre-matrix interfacial properties, with a predominant influence established by the weaker subject.
Studies focusing on fibre-matrix adhesion quality in radiation cured FRP composites have usually limited mechanical characterisation analyses to the Short Beam Shear test (SBS) and, to a less extent, the Three Point Bending (TPB) of $[90°]_n$ beam samples [9-12]. Although both tests are known to exhibit good correlation between the fibre-matrix Inter-Facial Shear Strength (IFSS) and the composite strength properties (the Inter-Laminar Shear Strength, ILSS, for the SBS, and transverse flexural strength for the TPB) [13,14], one further reason for the popularity of these mechanical characterisation tests is their ease of implementation. It is well known that fibre-matrix adhesion performances can play an important role also on the interlaminar fracture behaviour [13,15], which is well modelled in brittle FRP composites by the toughness parameters of Linear Elastic Fracture Mechanics (LEFM) [16].
The present study proposes the use of interlaminar fracture delamination as a main mechanical characterisation tool to evaluate unidirectional CFRP flat panels manufactured by means of a fast e-beam radiation curing technique. Mode I fracture toughness behaviour was investigated by means of Double Cantilever Beam (DCB) delamination tests, and Dynamic Mechanical Thermal Analysis (DMTA) on [0°] and [90°] beam samples were also performed to assess the curing degree of the resin matrix. The correlation of results from the proposed characterisations has shown new potentials for a more thorough investigation of structure/properties relationships in radiation cured composites.

2. Material systems and samples preparation

Two flat laminate plates with approximate dimension 20×25 cm^2 have been manufactured with the purpose to cut and test DCB samples according to ASTM D 5528. The nomenclature used to identify samples will be *pxy*, with *x* identifying the panel number and *y* the sample cut from the *px* panel. The main difference between the two panels is the presence of 10phr of a toughening PES monomer on the matrix system used in panel *p2*.

2.1 Selection of raw materials

The epoxy monomer was 2,2-bis[4-(glycidyloxy)phenyl]propane (DGEBA) by Aldrich and the initiator was an iodonium salt, cumyltolyliodonium tetra(pentafluorophenil) borate (Rh 2047), supplied by Rhodia Silicones. The toughening agent was an OH terminated polyethersulfone engineering thermoplastic, SUMIKA EXCEL 5003P, Mw 25,000, produced by Sumitomo Chemicals (Japan). Proportions of constituents in the resin blends are reported in table 1. In the toughened resin batch (panel *p2*) 10 phr of PES monomer powder was fully dissolved in the resin by keeping this at 120 °C for one hour under mechanical stirring. The resulting blend was then cooled and maintained at 80 °C to keep viscosity sufficiently low for fibre impregnation.
A dry fabric SikaWrap®-400C Mid Mod (Supplied by SIKA Italia) was used as reinforcement. This is a unidirectional carbon fibre crimped textile with fibre bundles hold together by waving weft nylon ties (se fig. 1a). The fabric had a nominal areal weight of 400 g/m^2 and employed high modulus carbon fibers (nominal E_f=390 MPa).

2.2 Laminates assembly

The manufacturing procedure of the carbon fibre reinforced (CFRP) panel consisted of two main steps: the pre-impregnation by hand lay-up of the fabric plies, and the radiation curing after opportune placement and exposure of the mold under the pulsed e-beam. The hand lay-up lamination followed a sequence of 8 aligned plies ($[0°]_8$), and was performed upon an aluminum plate (fig. 1), previously coated with liquid wax to ease the release of the cured composite. A second aluminum plate was placed on top of the laminate, and pressed by means of metallic clamps along the sides of the mold (see fig. 1b). The moderate applied pressure from the clamps helped to achieve a good surface finish and uniform thickness, but was not sufficient to consolidate the final laminate to high values of fibre volume fraction (V_f). In fact V_f of the composites after curing ranged between 34-39 %, which are typical figures expected for low pressure consolidated FRP laminates. During the hand-lay-up assembly a crack front was created by laying a a thin aluminium film (13 μm thickness). This was placed perpendicular to the fibres, along one edge of the panel and at the mid-section (see fig 1b).

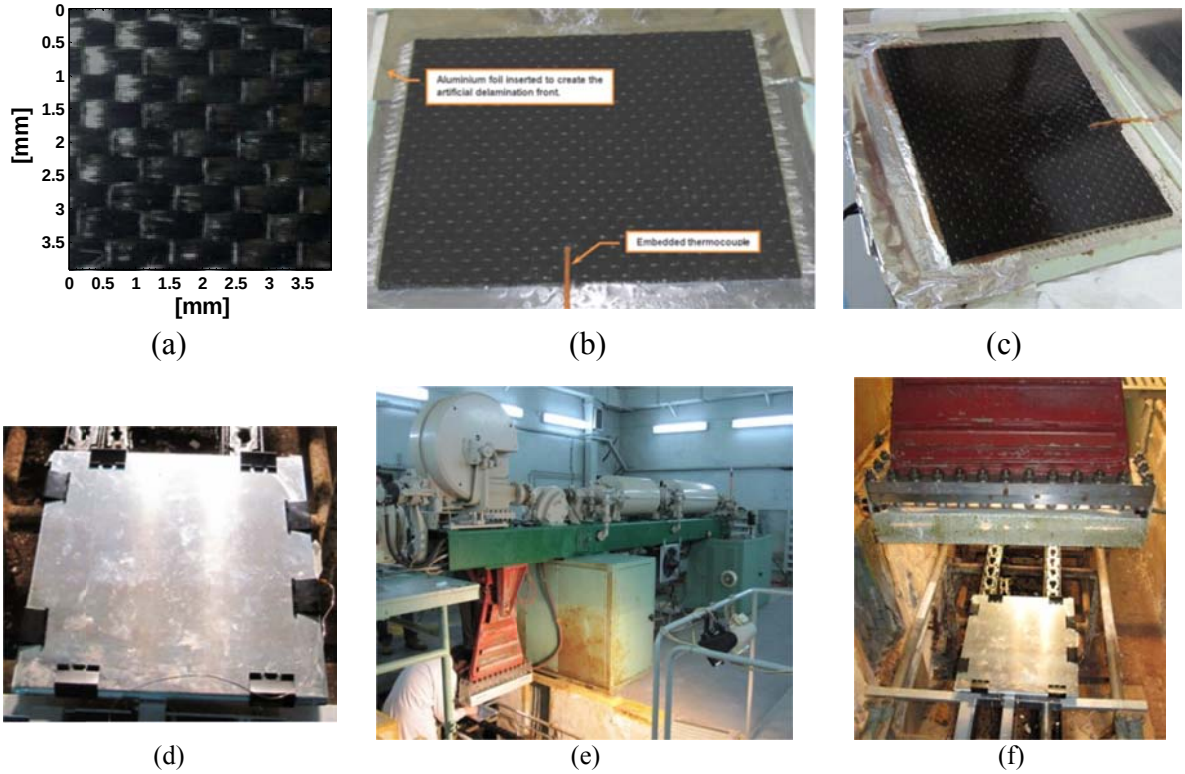

Figure 1. a) morphology of fabric texture; b) panel after impregnation and before placement on the radiating site; c) the cured panel being de-moulded; d) the closed mould; e) e-beam accelerator and placement of the mould; f) the mould on the conveyor belt under the e-beam gun shooter.

2.3 E-Beam curing

The e-beam irradiation of the blends has been realized using the LAE 10 MeV linear, pulsed accelerator located in the laboratory of the *ICHTJ* (*Inst. of Nuclear Chem. and Tech.*) of Warsaw. The aluminum mould containing the previously impregnated uncured composite laminate was fixed on a conveyor in a horizontal position under the pulsed electron beam gun (fig.1d,e,f). During irradiation the mould moves back and forward under the swiping electron beam. The temperature of the sample during irradiation was monitored through a thermo-resistor dipped into the resin (a little tube is embedded on one side of the wet laminate, see fig

1b, and the transducer wires are inserted through it). Every time the temperature transducer passes under the electron beam, a temperature peak is recorded (fig. 2).
The total irradiation dose, number of passes and other setting parameters are summarized in table 1. It is pointed out that panels *p1* and *p2* received about the same total dose rate (around 80 kiloGray). Panel *p2* though was irradiated at a higher dose rate, reducing the number of passes from 16 to 8 and the total curing time from 40 to 20 minutes. The different process parameters gave rise to two different thermal profiles as shown in figure 2.

Panel ID	Lay-up	PES [phr]	Iniziator [phr]	Total Dose [kGy]	Number of passes	Dose/pass [kGy]	Frequency [Hz]	Current [μA]
1	$[0°]_8$	0	0,5	80 kGy	16	5 kGy	38 Hz	0.63
2	$[0°]_8$	10	1,0	87 kGy	8	10 kGy	75 Hz	1.26

Table 1. Features and process data of the two composite laminate panels manufactured.

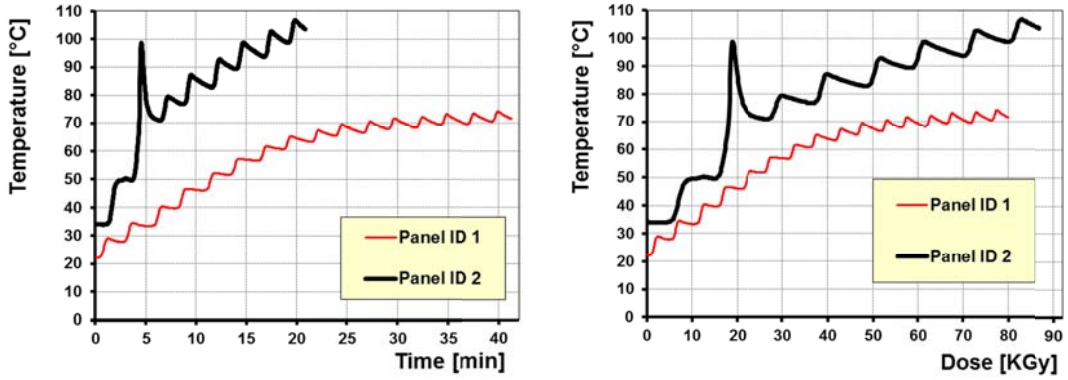

Figure 2. Temperature *vs.* time (left) and temperature vs. emitted radiation energy (right) plots.

2.4 Samples preparation

DCB samples were obtained by slicing rectangular stripes of nominal dimensions 20×140 mm^2 along the reinforcement direction. Metallic hinges were glued at the delaminated end of each beam to allow for gripping on the testing machine. The initial crack length had nominal value of 30 mm, oscillating by a value of ±1mm. It was found that DCB samples dimensions were compliant with the size equation criteria given in ASTM D 5528 (see table 2 for a data summary of the tested samples).

Sample ID	panel ID	Post curing	E [Gpa]	V_f % (st. dev)	Width B [mm]	Thickness h [mm]	Length L [mm]	a_0 [mm]
P11	1	no	110	39,8 (±0,7)	20	4,3 (±0,1)	140	30
P12			114					
P13			117					
P1p1		2 hours @ 130 °C	113					
P1p2			112					
P21	2	no	97	33,9 (±2)		3,95 (±0,2)		
P22			89					
P23			90					
P2p1		2 hours @ 130 °C	78					
P2p2			86					

Table 2. Samples nomenclature and properties. E is the flexural Young's modulus, and V_f is the fibre volume fraction. All other geometric symbols are used according to ASTM D 5528.

A thermal post-curing cycle after irradiation was also performed on some selected samples, in order to explore the possibility to complete the curing reaction of the irradiated materials. The conditions of this thermal treatment were 2 hours at 130°C, chosen on the basis of the DMTA data. The crosslinking density of all samples, post-cured and not, was investigated by deriving *tanδ* curves from DMTA tests as commented in section 3.1.

3. Experimental characterisation

3.1 Dynamic Mechanical Thermal Analyses (DMTA)

As evidenced in table 2, four different resin treatments have been obtained on manufactured samples: in the simply irradiated (*p1y* and *p2y* samples) and irradiate plus post-cured condition (*p1py* and *p2py* samples). Representative beam samples (30x8x*h* mm^3) from each curing condition were characterized through using a Rheometrics DMTA V instrument. Tests have been performed using a single cantilever bending set up, in temperature swift mode between 25-300 °C and a heating rate of 2 °C/min. The frequency was set to 1.8 Hz and the strain was 0.02 %. The loss factor (*tanδ*) vs temperature curves are shown in fig. 3. The glass transition temperature, T_g, was considered as determined by *tanδ* higher peak.

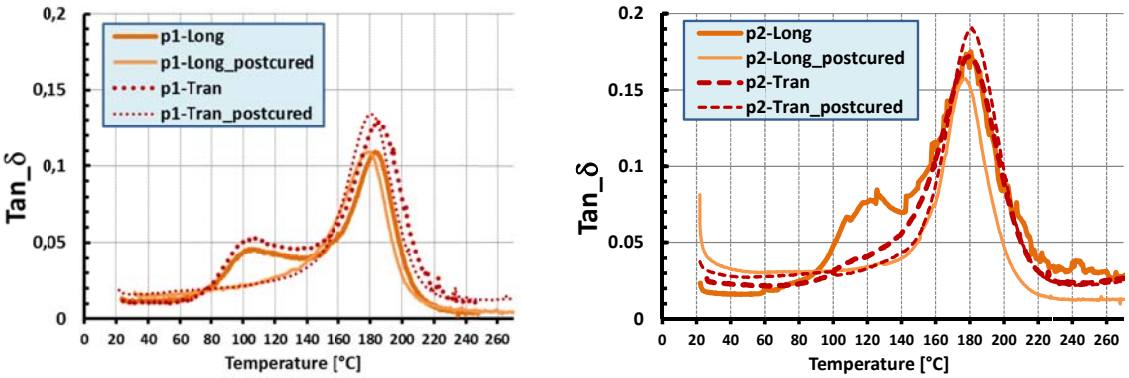

Figure 3. Plots of *Tanδ* vs Temperature. Long and Tran stay for longitudinal or transversal fibre direction with respect to the beam sample axis.

3.2 Fracture Toughness DCB tests

An electro-mechanical Instron 3367 testing machine was used to perform the DCB tests, measuring the Crack Opening Displacemt (COD) versus Load during the delamination growth (see fig. 4). The test was performed in displacement control at the constant machine crosshead speed of 3 mm/min. Crack extension was monitored by means of a video-camera and crack growth data opportunely synchronised with the measured load and COD. By following the classical data reduction procedures [15] it was then possible to obtain the critical Strain Energy Release Rate in mode I, G_{Ic}, and in particular the whole R-Curve monitoring the evolution of G_{Ic} with crack growth. Two parameters are finally considered for comparison of mechanical performances, i.e. the initial value of G_{Ic} at crack growth onset, G_{Icinit}, and the value of G_{Ic} when the R-Curve reaches a plateau, i.e. G_{Icprop}. Figure 4 shows an example of acquired data and the R-curve for sample *p11*, while all results are summarised in fig. 5. It is noted that a fully thermally cured system is added for comparison. This was produced with the same epoxy monomer and an amina DDS hardner (4,4'-Diaminodiphenyl sulfone), and used the same reinforcement fabric. It must be noted though that the thermal system was consolidated under high pressure, and its fibre volume fraction is much higher than that achieved by the irradiated systems. It is reported that a higher V_f usually has a beneficial effect on G_{IC} values and in particular on G_{IC_init} [13,15].

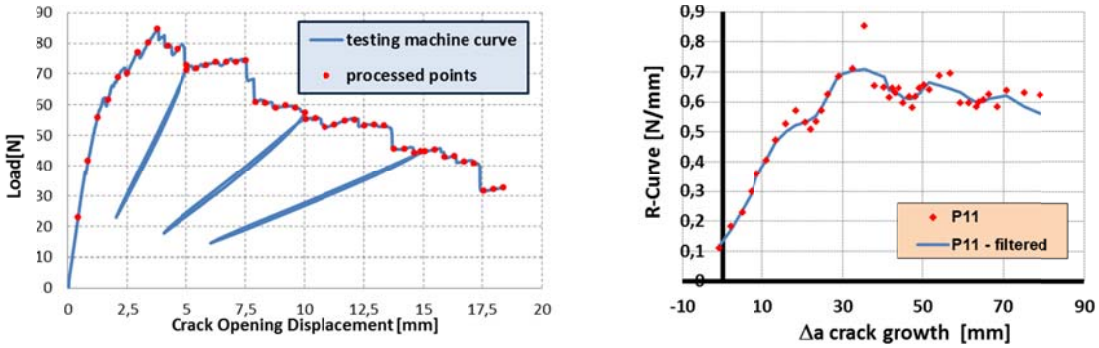

Figure 4. Acquired Load vs COD curve (left) and derived R-curve (right) on sample *p11*.

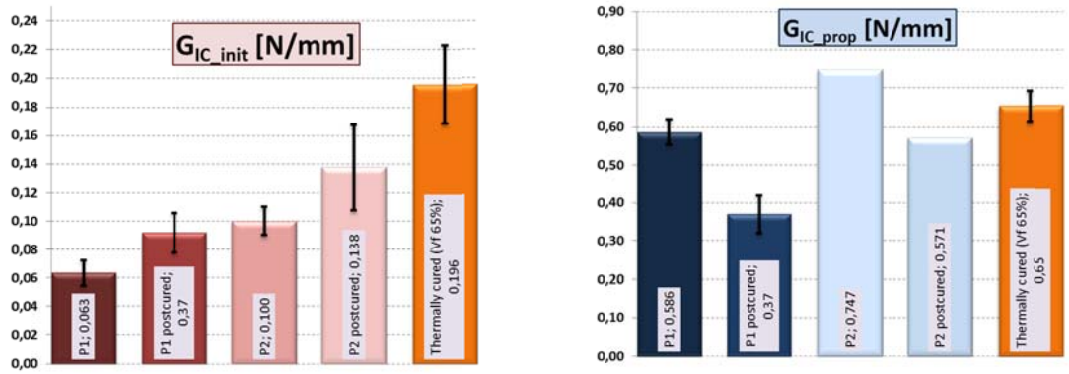

Figure 5. Critical Strain Energy Release Rate G_{IC} results.

4. Discussion of results

Although radiation curing does not need thermal activation, it can produce thermal effects on the samples due to both the exothermic polymerization reactions and the absorption heat by radiating energy. The choice of both the initiator concentration and the irradiation conditions, in terms of frequency, current and dose, is crucial in the resulting thermal history during the irradiation process (see fig. 2) [7,8,12]. In the present study the process temperature in sample *p1* does not exceed 77°C and it stays over 50°C for only 28 minutes, indicating a slight thermal treatment during irradiation. Sample *p2* had a higher initial temperature due to residual warmth of the mould which was heated to keep the Epoxy-PES system sufficiently fluid for lamination. Furthermore the higher dose/rate (or dose per pass [12]) gave rise to higher temperatures in the shorter curing cycle, which though did not exceed 100 °C.

Results of DMTA analyses in fig. 3 reveal that after irradiation, both samples produce two peaks, or a marked pre-peak shoulders, in the *tanδ* curves, correspondent to the relaxation of portions of the material at different cross-linking density. This effect, widely discussed by some of the authors in previous papers, is typical of blends irradiated at low temperature and is due to vitrification phenomena occurring during the cure reactions [17]. It is interesting to note that the *p2* panel has a less marked pre-peak shoulder (see for instance sample *p2-Tran* in fig. 3). This is likely due to the higher process temperatures which have assisted the curing kinetics inducing a more uniform crosslink density. The thermal post-cure has the effect to eliminate the pre-peak shoulder, but does not affect much the main peak (whose abscissa indicates the Glass Transition temperature, T_g). All systems show similar T_g values, around 180 °C, while the longitudinal beam samples usually exhibit lower *tanδ* peaks, probably due to a contribution of the fibres in keeping some stiffness after matrix relaxation. It is observed that the same value of T_g found for *Long* and *Trans* DMTA beam samples might have been

caused by a low fibre-matrix adhesion. In fact an effective fibre-matrix interface was expected to produce a higher T_g in the *Long* samples.
Results from the delamination tests are summarised in figure 5. Although samples *p2* have a slightly lower V_f, they exhibit a higher G_{ICinit} than *p1* due to the toughening effect of PES. Post-curing is found to increase G_{ICinit} on both systems. In this work the effect of post-cure is seen to enhance the crosslink density as discussed above. Although a higher crosslink density in bulk resins usually induce a lower fracture toughness (embrittling effect), in this case it gives a prevailing positive strengthening effect. The thermally cured system shows a higher crack onset critical energy, which is in large part due to the higher V_f.
In terms of crack propagation, the R-Curves have a rather marked initial growing trend, with a meaningful increase of the low values of G_{IC} (see fig. 6a). The higher values of propagation energy G_{ICprop} are in part due to the woven morphology of the fabric, and in part due to a marked fibre bridging density. Fibre bridging, i.e. fibres connecting the two fractured surfaces during crack propagation (see fig. 6b-c), is in general favoured by a poor fibre-matrix adhesion. Opposite to what observed with G_{ICinit}, a marked decrease is measured on the G_{ICprop} values of post-cured systems. This could be explained with an improvement of fibre/matrix adhesion induced by the thermal post-curing, which results in a decrease of fibre bridging density. Indeed a visual inspection of delaminating specimens (fig. 6b-c) seems to confirm that fibre bridging is higher in not post-cured specimen. Such effect of fibre/matrix adhesion improvement after thermal post-curing is also reported in [11]. It is also suggested for crack propagation, the embritlling effect of post-curing is now prevailing over the strengthening effect. The toughening effect of PES is also observed in the propagation stage, with values of G_{ICprop} higher in *p2* than *p1* for both post-cured and not post-cured samples. It is finally observed that propagation energy for irradiated and thermally cured systems is similar. The toughening mechanisms on crack propagation might though be different, with a prevailing fibre bridging effect in irradiated systems and a mechanical interlock between the dimples of the crimped fibre bundles in the more compacted (higher V_f) thermal system. It is expected that SEM analyses of cracked surfaces might reveal further indications of the fibre-matrix adhesion strength in the various systems, and its role in the delamination behaviour.

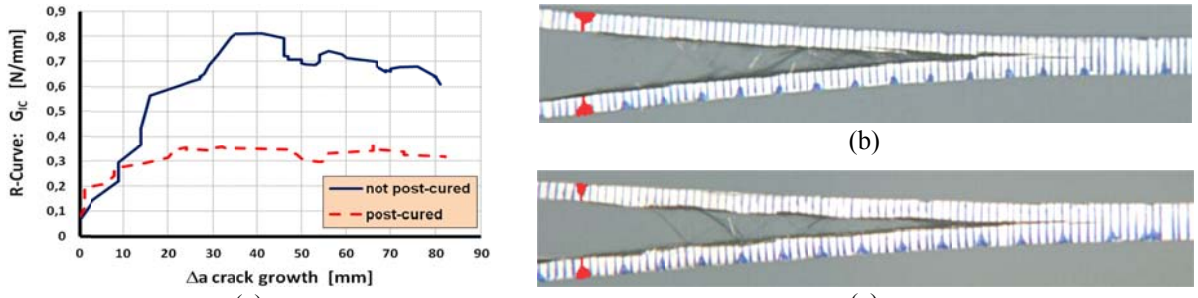

Figure. 6: a) typical R-Curves obtained from specimens *p11* and *p1p1*, and images of delaminations during crack propagation. The *p11* sample (b) shows a denser presence of fibre bridging than the *p1p1* sample (c).

5. Conclusion

Mode I interlaminar fracture toughness and DMTA analyses have been performed, and results correlated in order to evaluate the delamination behaviour of e-beam irradiated CF-epoxy composite laminates. Thermal post-curing has been found to have beneficial effects on critical initial crack resistance, and detrimental effects on propagation resistance, probably due to an improved fibre-matrix adhesion favouring less fibre bridging, and to an embrittlement of the matrix. In general fibre-matrix adhesion is believed to be strongly related with fibre bridging density and hence with crack propagation behaviour. The beneficial effects of blending epoxy

with PES has been confirmed in terms of enhanced critical delamination energies, both at initial and propagation stages. In general it has been found that the evaluation of the delamination behaviour with the traditional LEFM approach can be a valuable mechanical characterisation benchmark to investigate the role of matrix structural morphology and fibre-matrix adhesion strength of radiation cured FRP composites.

Acknowledgements
The authors would like to thank Dr. Grażyna Przybytniak of *ICHTJ (Warsaw-Poland)* and Dr. Marco Lavalle of *ISOF-CNR (Bologna-Italy)*, for their precious support in the manufacturing of the tested sample.

References

[1] Crivello JV. UV and electron beam-induced cationic polymerization. Nuclear Instruments and Methods in Physic Research B 1999;151:8-21.
[2] Lopata VJ, Saunders CB, Singh A, Janke CJ, Wrenn GE, Havens SJ. Electron beam-curable epoxy resins for the manufacture of high-performance composites. Radiation Physics and Chemistry 1999;56:405-15.
[3] Goodman DL, Palmese GR. Curing and Bonding of Composites using Electron Beam. In: Handbook of polymer blends & composites. Kulshreshtha AK and Vasile C, 2002; vol. 1-11, RAPRA Technology Ltd, 978-1-85957-309-6, Shropshire, UK.
[4] Berejka AJ, Eberle C. Electron beam curing of composites in North America. Radiation Physics and Chemistry 2002;63:551–556.
[5] Sui G, Zhong W-, Yang X-. The revival of electron beam irradiation curing of epoxy resin-materials characterization and supportive cure studies. Polym Adv Technol. 2009;20(11):811-7.
[6] Krzeminski M, Ponsaud P, Coqueret X, Defoort B, Larnac G, Avila R. Out-of-autoclave technologies for competitive high performance composites. In: International SAMPE Technical Conference; 2011.
[7] Alessi S, Dispenza C, Spadaro G. Thermal properties of e-beam cured epoxy/thermoplastic matrices for advanced composite materials. Macromolecular Symposia 2007;247:238e43.
[8] Alessi S, Dispenza C, Fuochi PG, Corda U, Lavalle M, Spadaro G. E-beam curing of epoxy-based blends in order to produce high-performance composites. Radiation Physics and Chemistry 2007;76:1308-11.
[9] Zhang Z, Liu Y, Huang Y, Liu L, Bao J. The effect of carbon-fiber surface properties on the electron-beam curing of epoxy-resin composites. Compos Sci Technol 2002;62:331–337.
[10] Eberle CC, Janke CJ, Sands JA, Wilenski MS. Interfacial properties of electron cured composites. Cooperative Research and Development Agreement Final Report for Cooperative Research and Development Agreement number ORNL99-0544; January 2005.
[11] Vautard F, Fioux P, Vidal L, Schultz J, Nardin M, Defoort B. Influence of the carbon fiber surface properties on interfacial adhesion in carbon fiber–acrylate composites cured by electron beam. Compos Part A 2011;42:859–867.
[12] Raghavan J. Evolution of cure, mechanical properties, and residual stress during electron beam curing of a polymer composite. Compos Part A 2009;40(3):300-308.
[13] Drzal LT, Madhukar M. Fibre-matrix adhesion and its relationship to composite mechanical properties. J Mater Sci 1993;28:569-610.
[14] Hoecker F, Friedrich K, Blumbergh H, Karger-Kocsis J. Effects of fiber/matrix adhesion on off-axis mechanical response in carbon-fiber/epoxy-resin composites. Compos Sci Technol 1995;54:317-327.
[15] Albertsen H, Ivens J, Peters P, Wevers M, Verpoest I. Interlaminar fracture toughness of CFRP influenced by fibre surface treatment: Part 1. Experimental results. Compos Sci Technol 1995;54/2:133–145.
[16] Fracture testing method for polymer, adhesives and composites (Moore D.R., Pavan A., Williams J.G., eds.). ESIS Publication No. 28, Elsevier (2001).
[17] Alessi, S., Calderaro, E., Parlato, A., Fuochi, P.G., Lavalle, M., Corda, U., Dispenza, C., Spadaro, G., 2005. Ionizing radiation induced curing of epoxy resin for advanced composites matrices. Nucl. Instrum. Meth. B 2005;236(1-4):55-60.